Non-monotonic phase behaviour of a mixture containing non-adsorbing particles and polymerising rod-like molecules

Thiyam, Priyadarshini; Woodward, Clifford E.; Forsman, Jan

Published in:
Journal of Colloid and Interface Science

DOI:
10.1016/j.jcis.2020.02.020

2020

Non-monotonic phase behaviour of a mixture containing non-adsorbing particles and polymerising rod-like molecules

Priyadarshini Thiyam

Division of Theoretical Chemistry, Lund University, P. O. Box 124, SE-221 00 Lund, Sweden

Clifford E. Woodward

School of Physical, Environmental and Mathematical Sciences, ADFA, Canberra, ACT 2600, Australia

Jan Forsman

Division of Theoretical Chemistry, Lund University, P. O. Box 124, SE-221 00 Lund, Sweden

Abstract

Hypothesis: Previous works have shown that many-body interactions induced by dispersants with increasing correlation length will generate a diminishing two-phase region [Soft Matter **14**, 6921 (2018)]. We conjecture that the attenuation of the depletion attraction due to many-body interactions is a ubiquitous phenomenon in medium-induced interactions. We propose mixtures of colloidal particles and rod-like polymers as a feasible experimental system for verifying these predictions, since the intra-molecular correlations are not screened in a good solvent for rod-like polymers as they are in flexible polymers. The length of the rods can grow and become the dominant length scale that determines the range of the depletion interactions for the imbedded non-adsorbing particles.

Simulations: We study many-body depletion forces induced by polymerizing rod-like polymers on spherical non-adsorbing colloids, using Metropolis Monte Carlo simulations. We also employ a simple mean-field theory to further justify our numerical predictions.

Findings: We demonstrate that the phase diagram displays the same qualitative features that have previously been predicted by many-body theory, for mixtures containing flexible polymers under theta solvent conditions. The contraction of the particle two-phase region that we observe, as the correlation length increases beyond some specific value, could be a signature of the weakening of the depletion caused by many-body effects.

Keywords: Depletion interaction; particle-rod mixture; many-body effects

1. Introduction

In a polymer particle mixture, depletion of (non-adsorbing) polymers from the interstitial regions between the particles leads to an attraction between them [1]. For polymers in the the Θ regime, a theoretical description of this depletion force was first given by Asakura and Oosawa [2, 3]. Their theory is applicable when the particle radius, R_s, is much larger than the polymer radius of gyration R_g (the *colloidal regime*). As the polymers obey Gaussian statistics, the characteristic length-scale of the 2-body interaction between a pair of spherical particles is R_g and, in the colloidal regime, the total contribution to the free energy due to depletion can be well-approximated by just 1- and 2-body terms (we denote this the *pair approximation*) [4, 5]. In the opposite case of relatively smaller particles, usually denoted the *protein regime*, it is well-known that the pair approximation is no longer valid and many-body (greater than 2-body) interactions become important. Extending the theoretical description to account for many-body interactions is quite a complex task, even for simple Gaussian polymers. [6, 1, 8].

Depletion forces are part of a much wider class of so-called medium induced interactions, also known as potentials of mean force (PMFs). Though that term is historically used to describe the interaction between just two particles (the 2-body interaction), its usage here will refer to the total free energy change in the dispersing medium, as it responds to the presence of fixed particles localized within it. Potentials of mean force are therefore thermodynamic in character,

containing energetic and entropic contributions. They have found application in systems such as polymer particle mixtures (as in the depletion interaction described above), charged colloids imbedded in electrolyte solutions and critical Casimir forces (CCFs). [9, 10, 11] CCFs have a range given by the correlation length of the dispersant, ξ, which diverges upon approach to the critical point and so many-body contributions to the free energy of the imbedded particles are crucial to include in that case.

In recent work, we showed that, for depletion interactions induced by equilibrium or *living* (and also polydisperse) Gaussian chains, the 2-body PMF approaches a $\sim 1/r$ dependence as the correlation length ($\xi \sim R_g$) diverges, where r is the particle separation.[12] Using such an interaction within the pair approximation would suggest that the total depletion contribution to the free energy per particle diverges. This is mathematically equivalent to the well-known thermodynamic non-integrability of systems interacting via the gravitational potential. By including the many-body interactions induced by the polymer dispersant these divergences are eliminated by significantly weakening the total depletion PMF. These many-body effects have a profound effect on other properties of the mixture, e.g., the phase separation induced by depletion interactions.[12]

Our expectation is that for many disparate types of medium induced interactions, the pair approximation will lead to similar unphysical behavior in the limit where the dispersant's correlation length becomes large, $\xi \to \infty$. That is, we believe that for many (if not most) scenarios, the 2-body PMF will become non-integrable in this limit. The depletion interaction described above for flexible polymers in the Θ regime is a case in point. Another example is provided by CCFs, where theoretical work has shown the 2-body PMF may give an algebraic decay, $\sim r^{-(1+\delta)}$, with $\delta \approx 0.04$ as one approaches the critical point of the dispersant [11]. Thus, in order to preserve sensible behavior of thermodynamic state functions (e.g. the chemical potential) in these regimes, we conjecture that the attenuation due to many-body interactions is a ubiquitous phenomenon in medium-induced interactions and a signature of this attenuation would be the narrowing of the particle two phase region as ξ increases beyond some specific

value.

Experimentally verifying this conjecture is possible but may lead to some difficulties. One scenario is suggested by our earlier work. In a dilute solution of equilibrium polymers, one could fix the total density of monomers as the size of the chains grow, approaching the polymerization transition. This may plausibly be accomplished by, e.g., manipulation of the chemical or physical conditions so as to cause the chains to elongate while the number of monomers remains fixed. However, as the polymer chains grow in length, the system will likely surpass the overlap concentration and one will no longer be in the Θ regime, which means that the chains cannot be treated as Gaussian. In this case, the range of the PMF will be determined by the monomer density as well, due to monomer-monomer interactions screening correlations. This will give a finite correlation length, $\xi << R_g$, as the average chain length diverges. A similar situation does not occur in the case of say CCFs, where the approach to the dispersant's critical point causes the correlation length (and range of the PMF) to diverge. In fact, significant work on CCFs have already shown that many-body interactions do appear to weaken the total critical Casimir interaction[13], which is consistent with the assertions presented here. This notwithstanding, it is our view that depletion interactions remain a robust and useful test-bed with which to investigate the behaviour of long-ranged PMFs, provided the screening problem can be overcome.

To this end, we propose an alternative depleting system that should not be subject to the screening effects described above and hence would provide a feasible experimental set-up with which to test the assertions above. We propose to revisit the already well-studied system of mixtures of rigid rods and spherical particles. In this case the intra-molecular correlations of the rigid rods are not screened by monomer-monomer interactions, no matter how long the rods become. Thus, the rod length can be increased so that it is the dominant length scale in the solution and will therefore determine the range of depletion interactions for imbedded (non-adsorbing) particles. The purpose of this work is to show that this system also displays the attenuation of the depletion interaction

via many-body interactions, as described above.

Despite the plethora of studies that have been carried out on this system (both theoretical and experimental) [14, 15, 16, 17, 18, 19, 20, 21, 22, 23, 24, 25, 26, 27, 28, 29, 30], the case of very long rods, has not been explicitly analyzed in terms of many-body contributions to the depletion interactions, in the way that will be highlighted in this work. Indeed, in some cases, previous theoretical work has indicated some uncertainty as to the role of many-body interactions in the long-rod regime [18, 21]. On the other hand, some seminal contributions already hint at the kinds of effects that we will make explicit here. For example, Bolhuis and Frenkel predicted a critical point at vanishing particle volume fraction for a mixture of particles and infinitely long rods [14]. This observation can be directly attributed to the many-body attenuation of the depletion interaction that we mentioned earlier.

In this study we will firstly carry out some theoretical analysis to outline the explicit role of many-body effects in the particle rod mixture, particularly in the limit of long rods. This will involve revisiting a well-known approximation based on scaled particle theory that implicitly contains many-body contributions within it. We will then describe the results of computer simulations of an explicit mixture of rods and spherical particles. Dealing with hard rods of finite diameter is computationally expensive, therefore we limit our study to infinitely thin rods. We anticipate that this model would still give qualitatively similar phase behavior for rods of finite width as the rod length becomes long. On the other hand, our approach precludes the possibility of liquid crystal transitions. Examples of experimental systems that this could represent include particle dispersions in tubular or fibrous polymeric structures with high rigidity and negligible affinity to the surfaces of the particles. The Tobacco Mosaic Virus and double-stranded DNA are also well-known potential dispersants with rod-like characteristics.

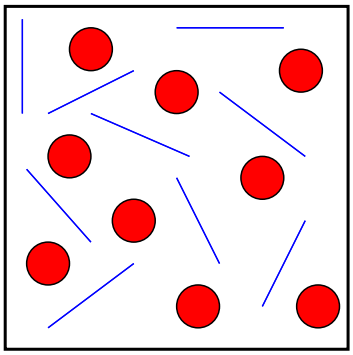

Figure 1: (Color online) Schematic figure of the system under consideration consisting of hard-sphere particles, dispersed in a solvent that also contains rod-like polymers.

2. Theory

2.1. The Pair Approximation for the Rod Particle Mixture

We consider N_S particles, which are modelled as hard spheres with a diameter d, imbedded in the rod solution,. The monodisperse rigid rods have length b and negligible width. Thus we model them as ideal rods with no mutual interactions though they are not permitted to cross any particle surface. The system is schematically illustrated in Figure 1. Before we describe our computer simulation studies of this system, it is instructive to consider some relations for the depletion interaction between the particles from the point of view of the many-body PMF.

We let $\Delta\omega^{(N_S)}$ be the free energy change of the initially pure rod solution upon inserting N_S spherical particles, whose fixed co-ordinates are confined to lie within a volume V_S. The number density of the spheres is therefore, $\rho_S = N_S/V_S$. We assume these are imbedded in a much larger volume V which contains N_{rod} rods, thus creating an osmotic equilibrium among the rods. As the rods are ideal they behave independently and the free energy of insertion is,

$$\beta\Delta\omega^{(N_S)}(\mathbf{R}^{N_S}) = -N_{rod}\ln\left[\int \frac{d\mathbf{r}}{V}\frac{d\omega}{4\pi}\exp(-\beta\Delta U(\mathbf{R}^{N_S},\mathbf{r},\omega))\right] \qquad (1)$$

Here $\mathbf{R}^{N_S}$ are co-ordinates of the fixed particles, while $\mathbf{r}$ describes a point on the rod (about which we measure its orientation ω) and β is the inverse thermal energy, $1/k_B\mathrm{T}$, with k_B Boltzmann's constant. The quantity $\Delta U(\mathbf{R}^{N_S}, \mathbf{r}, \omega)$ is the hard repulsion between the spherical particles and a rod. It is a sum of the individual rod-particle interactions,

$$\Delta U(\mathbf{R}^{N_S}, \mathbf{r}, \omega) = \sum_{i=1}^{N_S} \Delta u(\mathbf{R}^{(i)}, \mathbf{r}, \omega) \tag{2}$$

where $\mathbf{R}^{(i)}$is the position of the i^{th} sphere. Defining the Mayer function $F(\mathbf{R}^{N_S}, \mathbf{r}, \omega) = \exp(-\beta \Delta U(\mathbf{R}^{N_S}, \mathbf{r}, \omega)) - 1$, we can re-express the PMF as,

$$\beta \Delta \omega^{(N_S)}(\mathbf{R}^{N_S}) = -N_{rod} \ln \left[\int \frac{d\mathbf{r}}{V} \frac{d\omega}{4\pi} F(\mathbf{R}^{N_S}, \mathbf{r}, \omega) + 1 \right] \tag{3}$$

In the limit as $N_{rod}, V \to \infty$, $\rho_{rod} = N_{rod}/V =$ constant, we obtain,

$$\begin{aligned} \beta \Delta \omega^{(N_S)}(\mathbf{R}^{N_S}) &= -\rho_{rod} \int d\mathbf{r} \frac{d\omega}{4\pi} F(\mathbf{R}^{N_S}, \mathbf{r}, \omega) \\ &= \rho_{rod} V_{ex}(\mathbf{R}^{N_S}) \end{aligned} \tag{4}$$

where $V_{ex}(\mathbf{R}^{N_S})$ is the volume excluded to a rod by the spheres. This is the total depletion PMF. One can express the free energy as a sum of 1-, 2-body..n-body interactions,

$$\begin{aligned} \Delta \omega^{(N_S)}(\mathbf{R}^{N_S}) &= \sum_{i=1}^{N_S} \Delta \omega^{(1)}(\mathbf{R}^{(i)}) + \\ & \sum_{i=1}^{N_S} \sum_{j \neq i} \Delta \omega^{(2)}(\mathbf{R}^{(i)}, \mathbf{R}^{(j)}) + \ldots \end{aligned} \tag{5}$$

by using a systematic expansion of the RHS of Eq.(4) in terms of the single particle f-functions, $f(\mathbf{R}^{(i)}, \mathbf{r}, \omega) = exp(-\beta \Delta u(\mathbf{R}^{(i)}, \mathbf{r}, \omega)) - 1$ where,

$$F(\mathbf{R}^{N_S}, \mathbf{r}, \omega) = \prod_{i=1}^{N_S} (f(\mathbf{R}^{(i)}, \mathbf{r}, \omega) + 1) - 1 \tag{6}$$

For example, the 1-body PMF is given by,

$$\begin{aligned} \beta \Delta \omega^{(1)}(\mathbf{R}^{(i)}) &= -\rho_{rod} \int d\mathbf{r} \frac{d\omega}{4\pi} f(\mathbf{R}^{(i)}, \mathbf{r}, \omega) \\ &= \rho_{rod} (\gamma + \pi/6d^3) \end{aligned} \tag{7}$$

where $\gamma = \pi b d^2/4$ is the orientation weighted volume excluded to a rod by a single sphere (minus the sphere volume $(\pi/6)d^3$).

While the 1-body term is relatively easy to obtain, higher-body forces become more complex [24, 21]. An analysis by Roth [21] found that for large separation the 2-body potential appears to take the form,

$$\beta\Delta\omega^{(2)}(R) \sim -\rho_{rod} d^3 \mathcal{K}_1^*((R-d)/b) \tag{8}$$

where R is the distance between the centers of the spheres and $\mathcal{K}_1^*(x)$ is a dimensionless function. These 1- and 2-body contributions allow us to estimate the depletion free energy contribution for particle insertion via the *pair approximation* (described in the Introduction).

Focusing on long rods, $b/d >> 1$, we obtain for the 1-body term an insertion cost of $\sim \rho_{rod} b d^2$. The contribution due to 2-body interactions can be estimated by integrating the result of Eq.(8),

$$-\rho_S \rho_{rod} d^3 \int d\mathbf{R} \mathcal{K}_1^*((R-d)/b)\theta(|\mathbf{R}|-d) \sim -\rho_S \rho_{rod} b^3 d^3 \tag{9}$$

where $\theta(x) = 0$ (for $x < 0$) and unity elsewhere, is the Heaviside step-function. The 2-body term is negative and corrects for the overlap in the volume depleted of rods when many particles are present. We now consider increasing b, while the bulk rod density decreases so that $\rho_{rod} b$, and thus the 1-body contribution, remains fixed. On the other hand, the 2-body term increases without limit and will eventually dominate the 1-body contribution. Hence the pair approximation predicts that the depletion contribution to particle insertion becomes *negative*, which is clearly unphysical. Thus, the pair approximation fails in the long rod limit and one needs to account for the presence of many-body contributions.

The dominance of the 2-body term as the correlation length in the dispersant grows was also observed in the phase diagram of a particle dispersion, where the dispersant was a Θ solution of flexible (equilibrium) polymers with radius of gyration, R_g.[12] Depletion interactions will give rise to what can be described as a pseudo gas-liquid (G-L) phase transition of the particles. Using this analogy, we will by "gas" and "liquid" refer to the dilute and concentrated

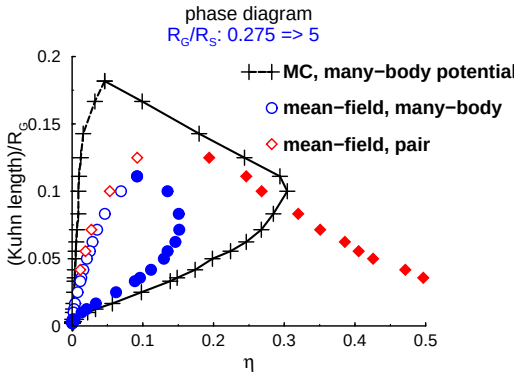

Figure 2: Phase coexistence for a mixture of ideal flexible polymers and non-adsorbing particles, as predicted by many-body theory. Data is taken from ref. [12] Coexistence data are given for a range of different polymer lengths, at a fixed monomer concentration. R_G denotes the radius of gyration of the polymers, whereas R_S is the particle radius. Lines are a guide to the eye. Plus signs are from Metropolis Monte Carlo (MC) simulations, utilizing a many-body Hamiltonian, whereas symbols without lines are from mean-field calculations [12]. Diamonds indicate mean-field data, where only the pair part of the many-body potential is used.

phases. We found that if $\rho_{pol} R_g^2$ is kept constant in the bulk polymer solution, while R_g increases, the 1-body depletion term remains finite, while the 2-body contribution diverges, similar to what we have just seen above in the case of rods. For the flexible polymers, however, we were able to obtain an accurate many-body PMF, which could be implemented in simulations. These simulations showed that the (G-L) portion of the phase diagram, plotted as a function of R_g^{-1}, displayed an upper critical point and a lower (cusp-like) termination point in the 2-phase region at zero particle density and $R_g^{-1} = 0$, see Figure 2. This was attributed to the weakening of the total depletion interaction arising from many-body effects. Also shown in Figure 2 are the results of a mean-field (MF) theory, which becomes essentially exact in the limit $R_g \to \infty$. The MF theory is also used to calculate the binodal that results from using only 2-body interactions in the PMF. That binodal displays an upper critical point but, erroneously, no lower termination of the 2-phase region. Instead, the 2-body PMF catastrophically overestimates the depletion attraction in the long polymer limit

($\sim 1/r$) and the liquid phase is only stabilized by the steric interactions between particles.

While we are not able to obtain an explicit many-body expression for the depletion PMF for rod-like polymers, we expect that those many-body contributions will have a similar effect on the phase diagram of the rod particle mixture. This will be demonstrated below using the "brute force" approach of simulating the *explicit* rod-particle mixture. This notwithstanding, it is possible to obtain some physical insight as to the role played by many-body interactions by considering an approximate perturbation approach [14, 15, 27] based on scaled particle theory.

2.2. Scaled Particle Theory: Many-body Effects

We begin by approximating the total depletion contribution to the free energy of the rod particle mixture using the following perturbation expression,

$$\Delta\Omega_{dep} \approx \ \rho_{rod} < V_{ex}(\mathbf{R}^{N_S}) >_0 \tag{10}$$

where $V_{ex}(\mathbf{R}^{N_S})$ is defined in Eq.(4) and $< ... >_0$, denotes an average over the configurations of the pure hard sphere fluid. It is convenient to write this in terms of, α, the so-called *free volume fraction*, $< V_{ex} >_0 = (1-\alpha)V_S$. A physically plausible approximation for α can be obtained from scaled particle theory (SPT), [14, 15, 27], which for infinitely thin rods gives

$$\alpha \approx (1-\phi_S)\exp(-\gamma\rho_S/(1-\rho_S)) \tag{11}$$

where $\phi_S = (\pi/6)\rho_S d^3$ is the free volume fraction of the particles. Substitution gives,

$$\beta\Delta\Omega_{dep} \approx \rho_{rod}(1-(1-\phi_S)\exp(-\gamma\rho_S/(1-\phi_S)))V_S \tag{12}$$

We now consider the high and low limits of the particle density (compared to γ^{-1}). In the low density regime, we obtain, $\alpha \approx 1-\phi_S-\gamma\rho_S$, and therefore

$$\beta\Delta\Omega_{dep} \to N_S\rho_{rod}(\gamma+\pi/6d^3) \tag{13}$$

which is just the sum of 1-body contributions, as expected. On the other hand, at high density we have,

$$\beta\Delta\Omega_{dep} \to \rho_{rod} V_S \tag{14}$$

In this density regime the SPT gives the physically sensible result that rods will be completely excluded from the volume occupied by the spheres. This leads to a simple "PV" expression for the depletion free energy, which is always positive. However, this is also the density regime where the pair approximation fails, predicting a negative depletion contribution (as illustrated above). We shall show below that a pair approximation obtained from the 1- and 2-body terms contained in the SPT also contains this problem, and it is instructive to see how many-body contributions, inherent in the full SPT expression, have conspired to correct this.

To do this, we expand the RHS of Eq.(12) as a power series in the particle density,

$$\beta\Delta\Omega_{dep} \approx N_S \rho_{rod} (\gamma + \pi/6 d^3 - \frac{1}{2}\frac{\gamma^2 \rho_S}{(1-\phi_S)} + \frac{1}{6}\frac{\gamma^3 \rho_S^2}{(1-\phi_S)^2} + ... \frac{1}{n!}\Delta\omega_{dep}^{(n)} \rho_S^{n-1} + ...) \tag{15}$$

This can be interpreted as a SPT approximation to the integrated many-body expansion, Eq.(5). Here the 1-body term is exact, as seen from Eq.(7), while the other n-body terms are approximated as,

$$\beta\Delta\omega_{dep}^{(n)} \approx (-1)^{n-1} \rho_{rod} \frac{\gamma^n}{(1-\phi_S)^{n-1}} \tag{16}$$

The denominator term involving powers of $(1-\phi_S)$ accounts for the pure hard sphere correlations between the particles. To see this, we consider $b \to \infty$ and $d^2 \propto 1/b$ so that γ remains constant. In this limit, the RHS of Eq.(15) remains a finite power series in ρ_S, while in the denominator, $\phi_S \to 0$. That is, as we allow the particles to become ideal, the rods become infinitely long so as to maintain a finite depletion contribution to the free energy, while removing steric correlations.

Inspection of Eq.(15) shows that the SPT predicts that the 2-body contribution scales as, $\sim \rho_{rod}\gamma^2$, rather than the presumably more accurate $\rho_{rod}\gamma^3$

as given in Eq.(9). However, both expressions predict that the 2-body term diverges as γ increases, while the 1-body contribution is kept fixed, implying failure of the pair approximation. Furthermore, the SPT indicates that *all* the individual many-body contributions will diverge under similar conditions, despite the fact that the free energy expression from which they were obtained remains well-behaved. The crucial parameter is the reduced density $R_v = \gamma\rho_S$, which is the ratio of the volume excluded to rods by particles and the average volume per particle. If R_v is small then the system can be treated as separate particles imbedded in the solution. If R_v is large, rods will generally be excluded from the volume V_S occupied by the particles. As the free volume fraction α will generally be (at least) a non-linear function of R_v, a many-body series for the free energy will contain terms of the type $\rho_{rod}R_v^n$ which will diverge for $n > 1$. While this has been shown explicitly within the SPT, we conjecture that this will be a general feature of any sensible many-body expansion of the depletion free energy for this system.

Thus, it seems that attempting to sum the total depletion free energy in terms of separate many-body contributions will fail in the long rod regime, as the resulting series will generally be outside its radius of convergence. Instead, a PMF approach to describe the rod-particle mixture would require one to obtain a full many-body expression that describes the correct limiting behaviours (embodied in Eq.(13) and Eq.(14)), rather than as a series of separate n-body contributions. While this was obtained for a dispersant of polydisperse Gaussian polymers [1], a many-body PMF for the case of stiff rods is still lacking. Therefore, we resort to simulations to illustrate the importance of many-body corrections to the pair approximation in the long rod limit.

3. Simulations

In our simulations we model the N_S particles imbedded in the rod solution as hard spheres with a diameter d. The monodisperse rigid rods have length b and are treated as ideal, with no mutual interactions, though they are not per-

mitted to overlap particles. We chose the bulk boundary conditions so that the 1-particle depletion contribution remained finite, while the rods were allowed to grow in length, i.e., $\rho_{rod}b$ remains fixed. This is equivalent to the total length of the rods (added together) remaining constant. If the rods consist of monomers which bond to form a rigid linear chain, then the bulk conditions imply a fixed total concentration of monomers in the bulk, as the degree of polymerization is increased. These conditions suggest an experimental scenario where system parameters that control the degree of polymerization of the rods, can be manipulated to increase the correlation length in the dispersing medium and hence the implicit range over which the depletion interactions will operate. To remain true to our model system, it is necessary to assume that the polydispersity in the rod length would remain relatively small, but this is unlikely to be crucial to the qualitative nature of the results we obtain below.

As shown above, under these conditions, the 1-body insertion free energy remains finite, while the 2-body and other separate n-body contributions to the depletion free energy will diverge as the degree of polymerization increases. This is an analogous system to that of the (flexible) Gaussian polymer particle mixture, discussed earlier, which gave the particle phase diagram in Figure 2. In that case, we held $\rho_{pol}R_g^2$ fixed, but as R_g^2 is proportional to the number of monomers per polymer, this is equivalent to holding the concentration of monomers in the bulk fixed. In that case the correlation length of the dispersant is proportional to R_g, whereas here the rod length, b, determines the correlation length. Our aim is to ascertain whether the peculiar lower termination of the G-L phase diagram (as depicted in Figure 2) also occurs in the particle rod mixture, indicating the many-body attenuation of depletion interactions in the long-rod limit.

In our simulations periodic boundary conditions were applied along all axes of the simulated cubic volume, with a side length L that was chosen to always exceed $2b$. We used Metropolis Monte Carlo (MC) to simulate this model. For the mixture and dispersant bulk separated by a virtual semi-permeable membrane, it is appropriate to perform simulations in the Semi-Grand Canonical

ensemble (s-GCMC) . However, we also present some results from Canonical ensemble simulations (CEMC), where the number of rods was held fixed.

As we intend to study the mixture for increasing b, the condition $L > 2b$ leads to computationally expensive simulations. Thus, a full determination of the G-L binodal would be numerically quite challenging. Therefore, rather than obtaining the complete binodal for the mixture, we set out to simply establish that the mixture displays the same *qualitative* features displayed in Figure 2. That is, an upper critical point and indications of a lower termination point of some description. To that end, we have found it expedient to instead just investigate the qualitative behavior of the particle-particle pair correlation function, $g_{SS}(r)$, as a function of the particle volume fraction ϕ_S $(= (\pi/6)N_S(d/L)^3)$ and use it to monitor the stability of the mixture. In particular (as noted in earlier work) the appearance of a long-ranged gradient in, $g_{SS}(r)$, on a lengthscale of the simulation box, provides a signature that the uniform system is becoming unstable, and undergoing phase separation. [1, 31]

In addition to the above calculations, we also performed simulations which utilized the pair interaction, $\Delta\omega^{(2)}(\mathbf{R}^{(i)}, \mathbf{R}^{(j)})$, between the particles, and compared the particle structures obtained with those of the explicit mixture simulation. We also explored another approximate form of PMF, which simplifies the interaction between rods and spheres. Both these studies are peripheral to the main aims of this paper and their results are presented and discussed in the Supplementary Information and will not be discussed further in the main part of the article.

4. Results and discussion

4.1. Canonical ensemble MC simulations

CEMC simulations provided some evidence for instability in the mixture as the rod length was increased. We considered the response of $g_{SS}(r)$ while ϕ_S was kept constant but the rod length was increased, at constant monomer density. That is, the density of the rods, ρ_{rod}, was decreased as b was increased so that

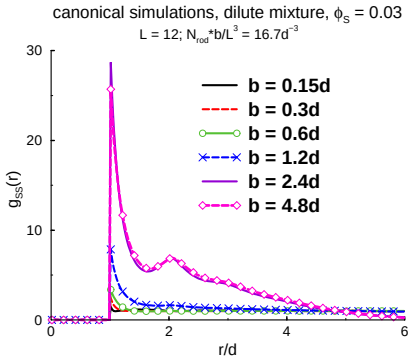

Figure 3: Particle-particle radial distribution functions ($g_{SS}(r)$) at $\phi_S \approx 0.0307$. Results from separate canonical simulations of mixtures containing monodisperse rods of length b are shown. In each case, the number of rods, N_{rod} is adjusted, so that $N_{rod}b(d/L)^3 \approx 16.67$.

$\rho_{rod}b$ was kept constant. As noted earlier, this mimics the experimental scenario of a supramolecular system wherein the number of monomers is fixed but the degree of polymerization is tunable. We initially considered 100 particles and 192000 rods of length $b \equiv 0.15d$, in a simulation box with fixed $L = 12d$ ($\phi_S \approx 0.03$) and then increased the rod length sequentially.

Figure 3 displays $g_{SS}(r)$ for different rod lengths. The strongest (primary) peak in $g_{SS}(r)$ initially increases with rod length, but otherwise shows very little structure in the fluid, which is typical for a low density gas phase. However, above some threshold value of rod length (in the range b =1.2d-2.4d), an instability sets in, as indicated by the long-ranged gradient in the tail of $g_{SS}(r)$. The growth of this tail is sudden and certainly not due to an increase in the correlation length, ξ ($\sim b$), in the dispersant. We also note that L remains significantly larger than b in this regime. Above $b \approx 2.4d$ or so, the primary peak of $g_{SS}(r)$ actually decreases with increasing rod length. This occurs due to the combined effects of a lower osmotic pressure from the rods as well as the presence of (repulsive) many-body effects that assert themselves with increasing rod length.

4.2. *Semi-grand canonical ensemble MC simulations*

In the CEMC simulations the density of monomers is fixed in the simulation volume. On the other hand, the system under study assumes the existence of a bulk dispersant in chemical equilibrium with the mixture, which required us to perform s-GCMC in order to model faithfully. As stated, we did not aim to map out full phase equilibrium curves, but only to verify that the rod/particle mixture has a qualitatively similar G-L binodal to that shown in Figure 2. In particular, we sought to show that, for a particle density greater than the upper critical isochore, the mixture demonstrated the following re-entrant behavior as the rod length was increased:

[single phase] $->$ [phase-separated] $->$ [single phase],

In s-GCMC simulation, we need to specify the chemical potential of rods in the bulk reservoir. At constant monomer density in the bulk, the density of rods decreases inversely with their increasing length, thus the chemical potential, μ, can be written in the following form,

$$\beta\mu(b) = \beta\mu_{ref} - \ln[\frac{b}{b_{ref}}] \tag{17}$$

where μ_{ref} is the chemical potential for a bulk rod solution with (arbitrarily chosen) length b_{ref}. For a given particle density, the successful insertion of rods becomes more unlikely as they become longer and thus, for convenience, we wanted to study a regime where rods do not become too long. We used preliminary simulations to establish that $b_{ref} = 45d$ and $\beta\mu_{ref} = -1$ gives an upper critical point for rods of reasonable length. For example, the mixture containing rods of length $b = 19.2d$ and $\phi_S \approx 0.12$ displayed only a single phase but underwent demixing for a range of lower particle volume fractions. This is shown in Figure 4 where we plot intermediate $g_{SS}(r)$ over the progress of a single s-GCMC simulation with rods of length $b = 19.2d$. Initially prepared as a homogeneous mixture of particles, with $\phi_S \approx 0.06$ this mixture spontaneously separated into L and G phases, as indicated by the growth of a long-ranged tail

in $g_{SS}(r)$. On the other hand, if we began these simulations with $\phi_S \approx 0.12$ in separate L and G phases, the system becomes uniform. In other words, the phase boundary for rods of length $b = 19.2d$ (which we arbitrarily denote as *long*) is located at a particle density in the range $0.06 < \phi_S < 0.12$.

This can be contrasted with the phase behavior with rods, of intermediate length, $b = 9.6d$. Figure 5, demonstrates that an initially uniform mixture containing these rods and a particle density of $\phi_S = 0.12$ will spontaneously phase separate. Hence, the phase boundary for intermediate rods is at a higher density than for long rods. This is in qualitative agreement with the lower part of the phase diagram depicted in Figure 2. That is, it appears that the 2-phase demixing region contracts as the length of rods increases. In the limit where the rod becomes very long, many-body interactions reduce the effective attractions between particles. We argue below, that the two phase region will likely terminate as a cusp in the limit $b \to \infty$, as happens in Figure 2. If the depletion PMF were pairwise additive, the demixing region would *increase* with rod length. This is seen in the short rod regime, where the pair contribution will dominate the overall PMF between the particles. In Figure 6, we see that as the rod length becomes shorter there will be no demixing at all for a particle density of $\phi_S \approx 0.12$, which is consistent with an upper critical point.

In Figure 7, we present an approximate stability diagram, at a particle density of $\phi_S \approx 0.12$, as obtained for a range of different rod lengths. The empty markers indicate phase separation, which we observed for intermediate rod lengths, while the filled markers represent the single phase regimes found at the short and long rod limits. We have also indicated (dashed line) an approximate binodal for such a polymerizing system.

4.2.1. Structural analysis of homogeneous and phase-separated systems

Here we confirm that the presence of the long-ranged gradient in $g_{SS}(r)$, corresponds to systems which display a clear tendency to phase separate. In Figure 8 we show configurations taken from the s-GCMC simulations of long and intermediate length rods, at $\rho_S \approx 0.12$. Figure 8(a) shows a single phase

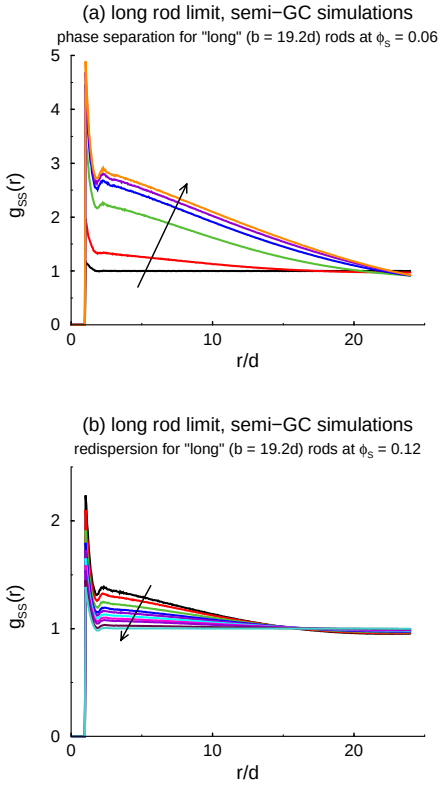

Figure 4: Particle-particle radial distribution functions from semi-grand canonical simulations (see text for details), at two different particle concentrations, with rods of length $b = 19.2d$. The curves show the simulations at different MC cycles, and the arrows indicate the progress of simulation towards equilibrium.

(a) $\phi_S \approx 0.06$.

(b) $\phi_S \approx 0.12$

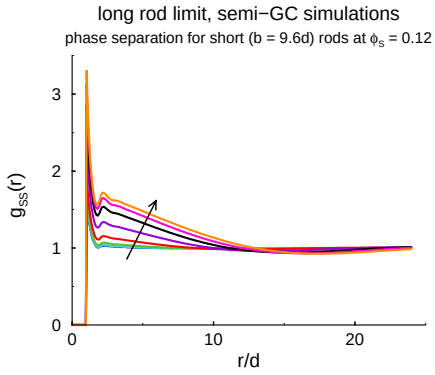

Figure 5: Particle-particle radial distribution functions from semi-grand canonical simulations, at $\phi_S \approx 0.12$, with rods of length $b = 9.6d$.

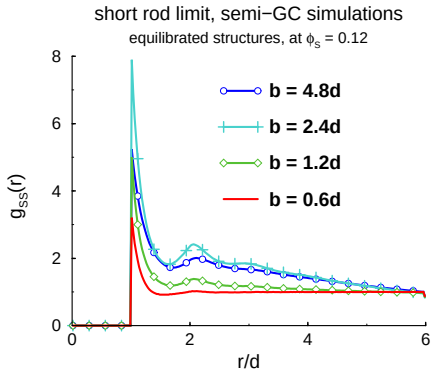

Figure 6: Particle-particle radial distribution functions from semi-grand canonical simulations at $\phi_S \approx 0.12$, for rods of various length in the short rod (colloidal) limit.

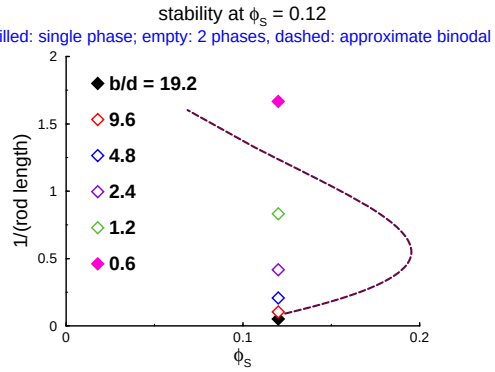

Figure 7: Phase behaviour, for rods of different lengths, at a particle density of $\phi_S \approx 0.12$. The filled markers, in the short and long rod limits, indicate that there is only a single phase. For intermediate rod lengths, there exists a phase separation, as indicated by the empty markers. The dashed curve traces an approximate binodal.

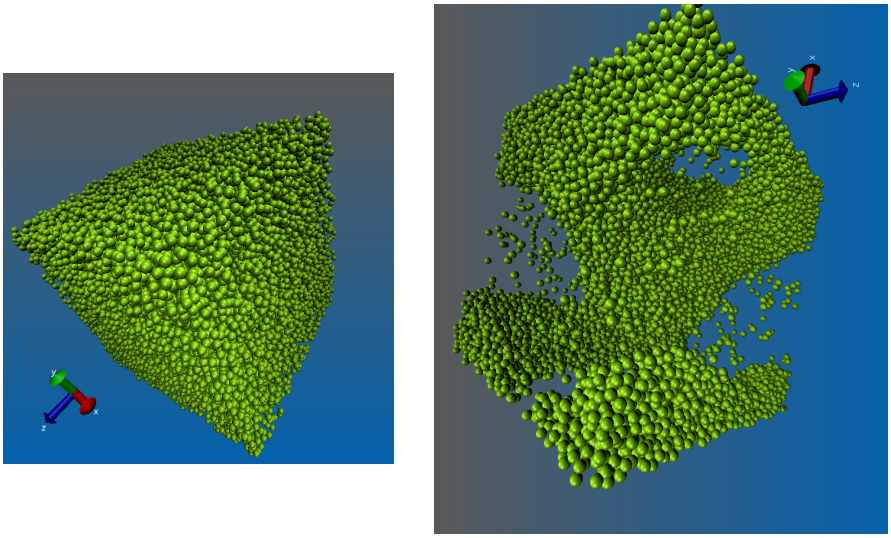

Figure 8: (Color online) Snapshots from semi-grand canonical simulations, at $\phi_S \approx 0.12$. The rods are not shown.

(a) $b = 19.2d$.

(b) $b = 9.6d$.

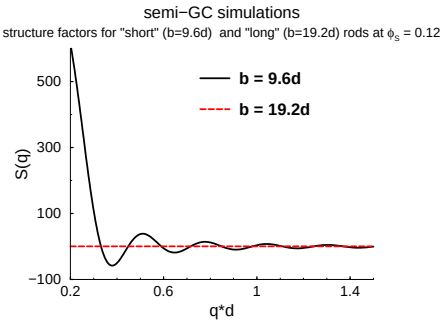

Figure 9: Structure factors, from semi-grand MC simulations at $\phi_S \approx 0.12$, in the presence of $b = 19.2d$ and $b = 9.6d$ rods, respectively). The displayed regime is limited to $qd > 0.2$, in order to avoid effects from periodic boundary conditions.

system with long rods wherein $g_{SS}(r) \approx 1$ over a large range of r (see Figure 4(b)). On the other hand, in Figure 8(b) there are voids of G phase, with a particle density lower than the average, interspersed in an L phase with higher than average density. The corresponding pair correlation is shown in Figure 5. When sampling to create $g_{SS}(r)$ in these phase separating systems, most near-neighbour pairs selected will be in the L phase, while a good proportion of distant pairs will have one particle in the L-phase and the other in the G-phase. This gives rise to a long-ranged slope in $g_{SS}(r)$.

It is important to note that these voided structures have not yet fully separated into separate L and G regimes, which requires a very large number of simulation steps for these large systems. Smaller simulations of demixing systems, which were run for a sufficiently long time, did display two separate L and G regions in the simulated volume. The interface between the phases were oriented parallel to one of the box sides due to a combination of surface area minimization and the periodic boundary conditions. In the Supporting Information, we display a snapshot of the complete phase separated structure. The approach towards these structures leads to a $g_{SS}(r)$ with a progressively more long-ranged tail as shown (for instance) in Figure 5.

For completeness, we show, in Figure 9, that phase separation can also be

traced by monitoring the structure factor, $S(q)$, (Fourier transform of $g_{SS}(r)$). However, this may require rather large systems, since we anticipate spurious effects from the periodic boundary conditions for $q < 4\pi/L$.

4.3. Scaled particle theory for lower termination point of G-L binodal

While in our simulations we did not explore the full phase diagram for the rod-particle mixture in the limit of very long rods. We can show, using the SPT that the G-L binodal is expected to display a lower cusp-like termination point, very similar to what is observed in Figure 2 for the flexible polymer case. Previous work using a similar approach has shown that a critical point can occur at zero particle concentration in the long rod limit [14], where ρ_{rod} was chosen as a thermodynamic variable. While that work did not consider the current boundary conditions (fixed $\rho_{rod}\gamma$), it does indicate that a phase coexistence does occur in the long rod limit at very low particle concentration.

We begin by writing the full free energy of the rod-particle mixture in the following (*generalized* van der Waals) form,

$$\Delta\Omega_{mix} = F_{id} + \Delta F_{HS} + \Delta\Omega_{dep} \tag{18}$$

The first term on the RHS of Eq.(18) is the ideal free energy of the separate particles and rods, the second term accounts for the hard sphere interactions between particles, and the last term accounts for the depletion contribution. We shall assume that the lower termination point will occur at very low particle concentrations ($\phi_S << 1$) allowing neglect the hard sphere contribution in Eq. (18). The free energy density ($\Delta\omega^*_{mix} = \beta\Delta\Omega_{mix}/V_S$) can then be written as a sum of ideal and depletion terms,

$$\Delta\omega^*_{mix} = \rho_S[\ln\rho_S - 1] + \rho_{rod}(1 - \exp(-\gamma\rho_S)) \tag{19}$$

where we have used the SPT approximation for the depletion contribution, Eq.(12), at low particle volume fraction. We now ascertain if this system is able to phase separate at these low densities, by investigating the spinodal curve. Substituting, $z = \rho_S\gamma$, we obtain,

$$\gamma\Delta\omega^*_{mix} = z[\ln z - \ln\gamma - 1] + \rho_{rod}\gamma(1 - \exp(-z)) \tag{20}$$

The spinodal is given by the condition,

$$\partial^2 \Delta\omega^*_{mix}/\partial z^2|_{z=z_{spin}} = 0 \tag{21}$$

which is easily solved to give the relation,

$$z_{spin} = \frac{\exp(z_{spin})}{\rho_{rod}\gamma} \tag{22}$$

We note that as, $\gamma \propto b$, if the bulk monomer density, $\rho_{rod}b$, is large enough , there are two spinodal points, $z^{(-)}_{spin}$ and $z^{(+)}_{spin}$. For fixed $\rho_{rod}b$, these solutions are independent of the rod length, b and thus the corresponding spinodal densities will then approach zero as linear functions of $1/b$, i.e., $\phi^{(-)}_{spin}, \phi^{(+)}_{spin} \sim 1/b$, which justifies our assumption of a low volume fraction (for large b) and that the 2-phase region will terminate as a cusp at zero density as $1/b \to 0$.

5. Conclusions

In this work, we have investigated a system of spherical non-adsorbing particles with rod-like polymers acting as depletants. Using MC simulations, we show that rod polymers with increasing length generate a shrinking two-phase region. This system displays qualitatively the same phase behaviour as found with depleting flexible polymers[12]. While the latter system must remain close to the θ point in order to display a diverging correlation length, ξ, the system with rod-like polymers can remain in the good solvent regime, while $\xi \to \infty$. Since there is clearly no screening of the intramolecular correlations in the rod, the range of the depletion interaction for the non-adsorbing particles is determined by the length of the rods, i.e., $\xi \sim b$. This type of system provides a more tenable experimental setting [30] for verifying the phase behaviour of particles that experience a many-body PMF, of diverging range, in a way that is akin to predictions in an earlier work [12] on particles+polymers in θ solvents. Some of the previous theoretical studies that have been conducted in this area, have suggested a rather modest role of many-body interactions in the long-rod regime [18, 21]. However, our study clearly demonstrates that such effects are quite substantial, at least in terms of how they affect the phase diagram.

Further, using a well-known perturbation expression for the free energy of the mixture, based on the SPT [14, 15, 27], we have been able to highlight major issues associated with treating such a system, by sequentially introducing a hierarchy of many-body interactions. Such an approach is expected to fail for long rods and one must instead use a PMF description that includes a *full* many-body description that properly describes the appropriate limiting behaviour. The effect of the many-body interactions is to diminish the depletion attraction as the rod length increases under the constraint of a constant monomer concentration. The results from earlier work, suggest that this constraint can be replaced by the more general requirement that the 1-particle component of the PMF remains finite [12], which is consistent with the mean-field analysis presented above. We assert that this type of many-body attenuation will be ubiquitous to medium-induced PMFs where the 2-body terms diverge in the $\xi \to \infty$ limit.

Recommended future work in this area include similar simulations, but where the rods have finite thickness. This would allow scrutiny of possible ways in which the phase diagram will change if the rods are prone to orientational self-assembly. Expanding the scope to adsorbing particles would also be interesting. Finally, it should be noted that our conjecture that CCFs in near-critical solvents will induce similar effects, where the anlogy to rod length would be correlation length, which in turn is given by the proximity to the critical point, remains to be verified, and quantified.

Acknowledgement

PT and JF gratefully acknowledge support from the Swedish Research Council.

Supporting Material available

In the Supporting Material, we describe how the pair potential of mean force used in our simulations is obtained. We further outline an alternative simulation

approach, utilizing excluded solid angles. Finally, we provide a snapshot of a small system that has phase separated.

References

[1] H. Lekkerkerker, R. Tuinier, Colloids and the depletion interaction, Lecture notes in physics, Springer, Germany, 2011. doi:10.1007/978-94-007-1223-2.

[2] S. Asakura, F. Oosawa, On interaction between two bodies immersed in a solution of macromolecules, The Journal of Chemical Physics 22 (7) (1954) 1255–1256. arXiv:https://doi.org/10.1063/1.1740347, doi:10.1063/1.1740347.
URL https://doi.org/10.1063/1.1740347

[3] S. Asakura, F. Oosawa, Interaction between particles suspended in solutions of macromolecules, Journal of Polymer Science 33 (126) (1958) 183–192. arXiv:https://onlinelibrary.wiley.com/doi/pdf/10.1002/pol.1958.1203312618, doi:10.1002/pol.1958.1203312618.
URL https://onlinelibrary.wiley.com/doi/abs/10.1002/pol.1958.1203312618

[4] A. P. Gast, C. K. Hall, W. B. Russel, Phase separations induced in aqueous colloidal suspensions by dissolved polymer, Faraday Discuss. Chem. Soc. 76 (1983) 189–201. doi:10.1039/DC9837600189.
URL http://dx.doi.org/10.1039/DC9837600189

[5] A. Gast, C. Hall, W. Russel, Polymer-induced phase separations in nonaqueous colloidal suspensions, Journal of Colloid and Interface Science 96 (1) (1983) 251 – 267. doi:https://doi.org/10.1016/0021-9797(83)90027-9.
URL http://www.sciencedirect.com/science/article/pii/0021979783900279

[6] A. I. Chervanyov, G. Heinrich, Potential theory of the depletion interaction in the colloid-polymer mixtures, The Journal of Chemical Physics 131 (23) (2009) 234907. arXiv:https://doi.org/10.1063/1.3273416, doi:10.1063/1.3273416.
URL https://doi.org/10.1063/1.3273416

[7] J. Forsman, C. E. Woodward, A simple many-body hamiltonian for polymer-colloid mixtures: simulations and mean-field theory, Soft Matter 8 (2012) 2121–2130. doi:10.1039/C2SM06737D.
URL http://dx.doi.org/10.1039/C2SM06737D

[8] H. Wang, C. E. Woodward, J. Forsman, Exact evaluation of the depletion force between nanospheres in a polydisperse polymer fluid under θ conditions, The Journal of Chemical Physics 140 (19) (2014) 194903. arXiv:https://doi.org/10.1063/1.4874977, doi:10.1063/1.4874977.
URL https://doi.org/10.1063/1.4874977

[9] E. J. W. Verwey, J. T. G. Overbeek, Theory of the Stability of Lyophobic Colloids, Elsevier, 1948.

[10] M. E. Fisher, P. G. de Gennes, Wall phenomena in a critical binary mixture, C. R. Seances Acad. Sci., Ser. B 287 (1978) 207–209.

[11] T. W. Burkhardt, E. Eisenriegler, Casimir interaction of spheres in a fluid at the critical point, Physical Review Letters 74 (16) (1995) 3189–3192. doi:10.1103/PhysRevLett.74.3189.
URL https://link.aps.org/doi/10.1103/PhysRevLett.74.3189

[12] H. S. Nguyen, J. Forsman, C. E. Woodward, Many-body depletion forces of colloids in a polydisperse polymer dispersant in the long-chain limit, Soft Matter 14 (2018) 6921–6928. doi:10.1039/C8SM00631H.
URL http://dx.doi.org/10.1039/C8SM00631H

[13] S. Paladugu, A. Callegari, Y. Tuna, L. Barth, S. Dietrich, A. Gambassi, G. Volpe, Nonadditivity of critical casimir forces, Nature Communications

7 (1) (2016) 11403. doi:10.1038/ncomms11403.
URL https://doi.org/10.1038/ncomms11403

[14] P. Bolhuis, D. Frenkel, Numerical study of the phase diagram of a mixture of spherical and rodlike colloids, The Journal of Chemical Physics 101 (11) (1994) 9869–9875. arXiv:https://doi.org/10.1063/1.467953, doi:10.1063/1.467953.
URL https://doi.org/10.1063/1.467953

[15] G. A. Vliegenthart, H. N. W. Lekkerkerker, Phase behavior of colloidal rod-sphere mixtures, The Journal of Chemical Physics 111 (9) (1999) 4153–4157. arXiv:https://doi.org/10.1063/1.479713, doi:10.1063/1.479713.
URL https://doi.org/10.1063/1.479713

[16] M. Schmidt, Density functional theory for colloidal rod-sphere mixtures, Phys. Rev. E 63 (2001) 050201. doi:10.1103/PhysRevE.63.050201.
URL https://link.aps.org/doi/10.1103/PhysRevE.63.050201

[17] P. Tian, G. D. Smith, Molecular dynamics simulations of nanoparticles in dense isotropic nematogens: The role of matrix-induced long-range repulsive interactions, The Journal of Chemical Physics 124 (18) (2006) 184701. arXiv:https://doi.org/10.1063/1.2196038, doi:10.1063/1.2196038.
URL https://doi.org/10.1063/1.2196038

[18] A. Esztermann, M. Schmidt, Density functional theory for sphere-needle mixtures: Toward finite rod thickness, Phys. Rev. E 70 (2004) 022501. doi:10.1103/PhysRevE.70.022501.
URL https://link.aps.org/doi/10.1103/PhysRevE.70.022501

[19] D. Antypov, D. J. Cleaver, Orientational and phase-coexistence behaviour of hard rod–sphere mixtures, Chemical Physics Letters 377 (3) (2003) 311 – 316. doi:https://doi.org/10.1016/S0009-2614(03)01157-6.
URL http://www.sciencedirect.com/science/article/pii/S0009261403011576

[20] D. Antypov, D. J. Cleaver, The role of attractive interactions in rod–sphere mixtures, The Journal of Chemical Physics 120 (21) (2004) 10307–10316. arXiv:https://doi.org/10.1063/1.1718181, doi:10.1063/1.1718181.
URL https://doi.org/10.1063/1.1718181

[21] R. Roth, Depletion potentials in colloidal mixtures of spheres and rods, Journal of Physics: Condensed Matter 15 (1) (2002) S277–S282. doi:10.1088/0953-8984/15/1/337.
URL https://doi.org/10.1088%2F0953-8984%2F15%2F1%2F337

[22] W. Li, T. Yang, H.-r. Ma, Depletion potentials in colloidal mixtures of hard spheres and rods, The Journal of Chemical Physics 128 (4) (2008) 044910. arXiv:https://doi.org/10.1063/1.2820785, doi:10.1063/1.2820785.
URL https://doi.org/10.1063/1.2820785

[23] L. Wu, A. Malijevský, G. Jackson, E. A. Müller, C. Avendaño, Orientational ordering and phase behaviour of binary mixtures of hard spheres and hard spherocylinders, The Journal of Chemical Physics 143 (4) (2015) 044906. arXiv:https://doi.org/10.1063/1.4923291, doi:10.1063/1.4923291.
URL https://doi.org/10.1063/1.4923291

[24] K. Yaman, C. Jeppesen, C. M. Marques, Depletion forces between two spheres in a rod solution, Europhysics Letters (EPL) 42 (2) (1998) 221–226. doi:10.1209/epl/i1998-00227-1.
URL https://doi.org/10.1209%2Fepl%2Fi1998-00227-1

[25] K.-h. Lin, J. C. Crocker, A. C. Zeri, A. G. Yodh, Colloidal interactions in suspensions of rods, Phys. Rev. Lett. 87 (2001) 088301. doi:10.1103/PhysRevLett.87.088301.
URL https://link.aps.org/doi/10.1103/PhysRevLett.87.088301

[26] W. C. K. Poon, P. B. Warren, Phase behaviour of hard-sphere mixtures, Europhysics Letters (EPL) 28 (7) (1994) 513–518. doi:10.1209/

0295-5075/28/7/010.
URL https://doi.org/10.1209%2F0295-5075%2F28%2F7%2F010

[27] S. K. Lai, X. Xiao, Phase diagram of colloid-rod system, The Journal of Chemical Physics 132 (4) (2010) 044905. doi:10.1063/1.3298993.
URL https://doi.org/10.1063/1.3298993

[28] M. Adams, Z. Dogic, S. L. Keller, S. Fraden, Entropically driven microphase transitions in mixtures of colloidal rods and spheres, Nature 393 (1) (1998) 349–352. arXiv:https://doi.org/10.1038/30700, doi:10.1038/30700.
URL https://doi.org/10.1038/30700

[29] G. H. Koenderink, G. A. Vliegenthart, S. G. J. M. Kluijtmans, A. van Blaaderen, A. P. Philipse, H. N. W. Lekkerkerker, Depletion-induced crystallization in colloidal rod-sphere mixtures, Langmuir 15 (14) (1999) 4693–4696. arXiv:https://doi.org/10.1021/la990038t, doi:10.1021/la990038t.
URL https://doi.org/10.1021/la990038t

[30] G. H. Koenderink, D. G. A. L. Aarts, V. W. A. de Villeneuve, A. P. Philipse, R. Tuinier, H. N. W. Lekkerkerker, Morphology and kinetics of phase separating transparent xanthan-colloid mixtures, Biomacromolecules 4 (1) (2003) 129–136, pMID: 12523857. arXiv:https://doi.org/10.1021/bm025633f, doi:10.1021/bm025633f.
URL https://doi.org/10.1021/bm025633f

[31] C. E. Woodward, J. Forsman, A many-body hamiltonian for nanoparticles immersed in a polymer solution, Langmuir 31 (1) (2015) 22–26, pMID: 25547161. arXiv:https://doi.org/10.1021/la5037184, doi:10.1021/la5037184.
URL https://doi.org/10.1021/la5037184

6. Simulations utilizing a pair potential of mean force

The impact of many-body effects can be illustrated by comparisons with analogous systems where only pairwise interactions operate. To this end, we first establish a reference pair potential, βw_{ref}, by working out how the excluded volume Γ varies with the separation between two colloidal particles in some volume V_1. V_1 is chosen large enough to avoid edge effects, but small enough to facilitate good statistics. A reference pair potential of mean force (PMF), w_{ref} can then be defined as:

$$\beta \Delta w_{ref} = \Gamma(S) - \Gamma(\infty). \tag{23}$$

We perform a canonical Monte-Carlo simulation of two colloidal particles and a single rod. Since the actual interaction free energy scales with the osmotic pressure, we work out the relation between the osmotic pressure Π_N in our full N-rod and many-particle system and the pressure Π_1 relevant to our single rod 2-particle system. Using

$$\Pi_1 = \frac{1}{V_1(1 - \Gamma(\infty))}, \tag{24}$$

and

$$\Pi_N = \frac{N}{V_N(1 - < \Gamma >_N)}, \tag{25}$$

where V_N is the volume of the N-rod many-particle system, and $< \Gamma >_N$ is the average rejection ratio in the many-particle system without any rods, we arrive at the final pair potential $\beta W_{pair}(S)$

$$\beta \Delta w_{pair}(S) = \frac{\Pi_N}{\Pi_1} \Delta w_{ref}(S) \tag{26}$$

This pair potential can then be utilised to work out structures in the many-particle system, under the assumption of a pair potential. In these N-body simulations, the colloidal particles only interact through Δw_{pair}. In the simulation, the excluded volume Γ is given by the insertion rejection ratio. The average rejection ratio $< \Gamma >_N$ in the many-particle system without rods is in principle dependent on the structures formed, but given that it is a quantity

that is typically of the order of 0.03, we have simply utilised a random configuration of particle-only simulation from which $< \Gamma >_N$ is obtained by random insertions using Widom's method.

Invoking these approximations, we can simulate our N particles with an implicit treatment of the rods, via the pair-PMF (Δw_{pair}) they are assumed to generate. We expect the pair-PMF approximation to be exact for short rods, but with a deteriorating accuracy for longer rods. This is indeed the case, as illustrated in Figure 10. One interesting observation is that the pair approximation is apparently accurate even when the rods length (slightly) exceeds a particle diameter. This is in contrast to the case with flexible (ideal) polymers [1]. Nevertheless, for b values exceeding 2 or so, the pair approximation deteriorates quite rapidly, as expected.

7. A rod-sphere potential of mean force determined by the amount of excluded solid angle

We derive an alternative rod-particle PMF based on the amount of solid angle that is excluded by the surrounding spheres to any single rod rotating about its centre. In a simulation, one can do this exactly by considering explicit rotations. We then invoke the approximation that the total solid angle excluded is obtained by summing over all spheres within the range of the rotating rod. This is a sum of (pair) terms between the rod and each of the n spheres that are within a rod length from our "tagged" end. The total "effective interaction" , U, between the rod and the surrounding spheres is then:

$$\beta U = -\ln\left(1 - \sum_{i=1}^{n} \frac{1}{4\pi} d\Omega_i\right), \tag{27}$$

where β is the inverse thermal energy, and $d\Omega_i$ is the solid angle excluded between a rod and sphere i. The excluded solid angle between the rod and a sphere for a given distance between rod centre and sphere centre is obtained analytically. The difference between the above expression and the exact explicit rod simulations utilized in the main paper is that not all of the spheres within

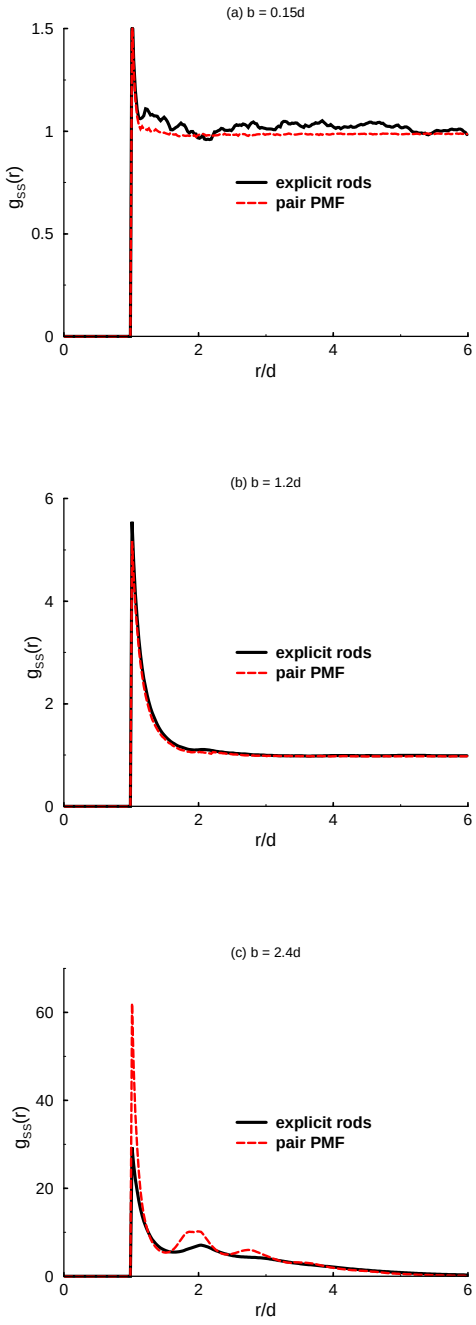

Figure 10: (Color online) Comparison of the pair PMF and explicit simulations for different rod lengths.

range of the rod will necessarily contribute to the sum. There may be some spheres which are shielded from impeding the rod by other spheres closer to the centre of the rod. This leads to an overcounting of the excluded solid angle, with the current approximation. In fact, at high sphere density it is theoretically possible that this over-counting leads to a total excluded solid angle that exceeds 4π. However, we have set an upper bound at 4π. For short rods (compared to the particle diameter) the solid angle approach is expected to be accurate. The accuracy of the solid angle approximation is evaluated in Figure 11. Obviously, this approach can only be used for systems in which the rods are smaller than the particles.

The simulation with the second type of POMF based on excluded volume agrees with data from explicit rod simulations for very short rods ($b = 0.15$). For $b = 0.6$ onwards, minor deviations begin to appear with the POMF simulations predicting a somewhat too strong structuring, which is expected, on account of the double counting that occasionally will take place for long rods. However, for even longer rods, this POMF approach predicts a much too weak peak for the sphere-sphere $g(r)$; see Figure 11. This is for cases where the explicit simulation generates a phase separation. This can be explained as follows: Consider the format of a slab of dense particles, along the z-direction (say). Also consider placing the end of a a long rod close to the planar interface of this dense phase. With the explicit method, the rod will have sacrificed half of its rotational entropy, compared to a reference bulk. But with the implicit method, the double counting can lead to an entropic price that is essentially infinite, which would imply the formation of vacuum slabs on either side to the dense phase. Forming such slabs will of course be quite expensive, which in practice prevents dense phases to form.

Another way of thinking about it in the uniform phase is that, for very long rods, the POMF approach underestimates the advantage of bringing spheres together (to minimise rotational entropy), as it over-counts the amount of excluded solid angle. The shadowing of one sphere by another is not accounted for in the POMF but, for long rods, it is one of the mechanisms that the sphere

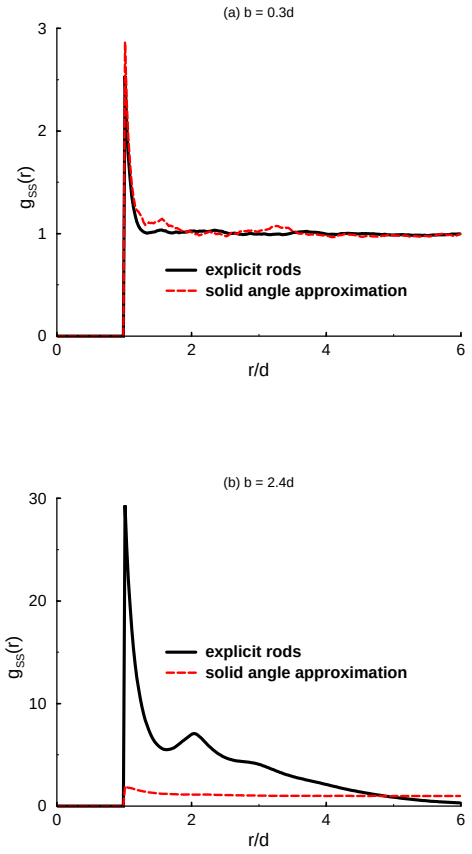

Figure 11: (Color online) Comparison of the excluded solid angle PMF and explicit simulations for different rod lengths.

configurations maximise rotational entropy, by bringing spheres together. For short rods this mechanism is not that important; many-body vs few-body again!

Simulations using this kind of interaction only involve a sum over pair terms, implying a high computational efficiency. However, determining the solid angle excluded and calculating the effective interaction given by eq. (27) for each pair of rod and sphere actually become a costly task. One has to compute U even for overlapping cases. We find that this approach is no less time consuming than the explicit simulations. In an explicit simulation, a detection of a particle overlap leads to an immediate rejection, which normally amounts to a truncation of the loop across the particles, and hence a computational saving.

8. Snapshot from a phase separated (rather small) system, near equilibrium

In Figure 12, we display a snapshot subsequent to a long simulation of a smaller system,that is otherwise (except size) identical to that shown in Figure 8 (b) of the main paper. The side length of this smaller system still exceeds to rod lengths, so we do not anticipate significant size effects to the fully equilibrated structure. In other words, the system displayed in Figure 8 (b) of the main paper is still approaching equilibrium conditions, which is also obvious from the progression of $g(r)$, shown in Figure 5.

[1] Forsman, J.; Woodward, C. E. A simple many-body Hamiltonian for polymercolloid mixtures: simulations and mean-field theory. *Soft Matter* **(2012)**, *8*, 2121-2130.

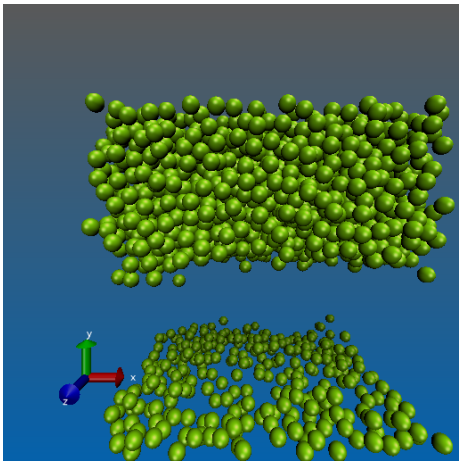

Figure 12: (Color online) Snapshot